GEOLOGICAL INSIGHTS INTO CHANDRAYAAN-2 LANDING SITE IN THE SOUTHERN HIGH LATITUDES OF THE MOON. Rishitosh K. Sinha[1], Vijayan Sivaprahasam[1], Megha Bhatt[1], Harish Nandal[1], Nandita Kumari[1], Neeraj Srivastava[1], Indhu Varatharajan[1,2], Dwijesh Ray[1], Christian Wöhler[3], and Anil Bhardwaj[1], [1]Physical Research Laboratory, Ahmedabad 380009, India (Email: rishitosh@prl.res.in), [2]Institute for Planetary Research, German Aerospace Center DLR, 12489 Berlin, Germany, [3]Dortmund Technical University, Image Analysis Group, Otto-Hahn-Str., 4, 44227 Dortmund, Germany.

Introduction: Chandrayaan-2 mission will be the third giant leap by the Indian Space Research Organisation (ISRO) in their continued planetary exploration program [1]. It is planned to be launched in early 2019. This mission will be realized in three phases that includes orbiting, landing and roving [1]. Successful implementation of the Chandrayaan-2 lander (named 'Vikram') and rover shall be attributed as the first-ever touchdown on the surface of lunar highlands at high southern latitudes.

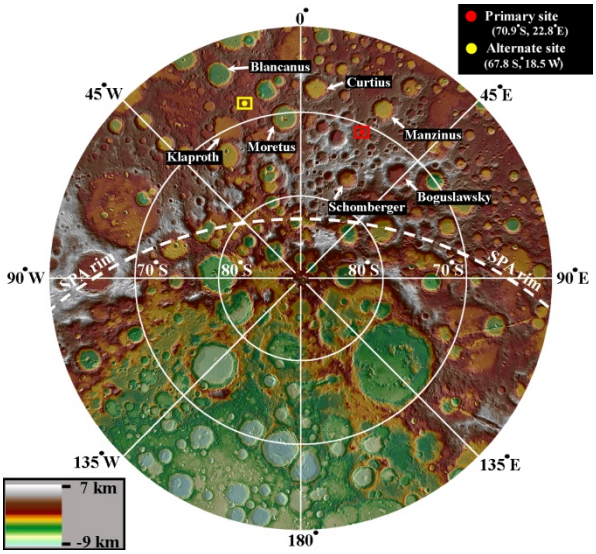

Figure 1. LRO WAC image mosaic overlaid on WAC GLD100 DTM showing the southern sub-polar region of the Moon. Both the primary (red circle within red box) and alternate (yellow circle within yellow box) landing sites are shown. Map is in polar stereographic projection. The dashed white line is the South Pole Aitken (SPA) basin rim.

The primary landing site (PLS; 70.9˚S, 22.8˚E) of the mission is located ~350 km north of the South Pole Aitken (SPA) basin rim (Figure 1) [2]. Subsequently, a 15 x 8 km ellipse is identified for landing within an area between 70˚ - 72˚ S and 22˚ - 24˚ E. Additionally, an alternate landing site (ALS) has also been selected at 67.8˚ S, 18.5˚ W (Figure 1) [2]. In this work, we have carried out detailed geological characterization of the landing ellipse of the PLS using remote sensing datasets to provide a contextual framework for in-situ investigations by the rover and lander instruments.

Observations and results: *Topography and morphology.* The slope map (Figure 2a) generated using LOLA topography data (~60 m/pixel) [3] reveals that ~94% of the area within the ellipse have slope within 15˚. The remaining 6% of the ellipse have locally steep slopes (>15˚) and are only associated with craters (Figure 2a). Morphological observations using LRO NAC (~0.5-1.5 m/pixel) images [4] suggest that the craters within the landing ellipse have morphologies varying from very fresh (consistent with bright rays), relatively fresh (consistent with rocks/boulders near the rims/walls), and degraded appearances (irregularly shaped rims and dominated by post-cratering events) (Figure 2b). Additional observations using the Kaguya TC DTM [5] and NAC images reveals evidence of ghost craters (incomplete rims) in the ellipse.

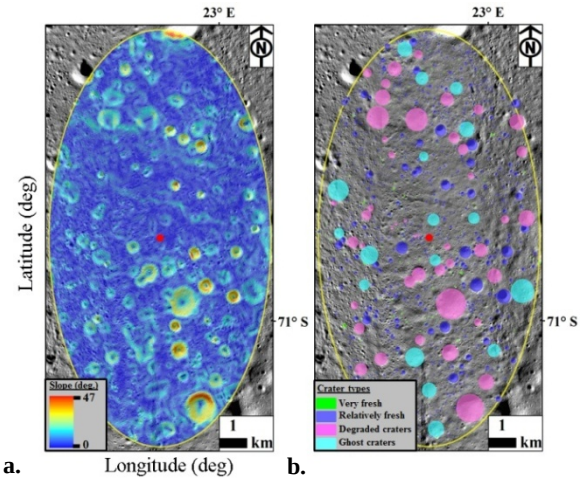

Figure 2. (a) LOLA topography data based slope map of the landing ellipse. **(b)** Morphology map of the landing ellipse showing the distribution of four types of craters observed within the ellipse. Background is the mosaic of LRO NAC images. In both figures, the red circle in the center shows the location of the PLS.

Crater distribution and age. The total count (23605) of craters within the ellipse using the NAC images reveals that there are 13600 craters whose diameter is >10 m and only 11 craters with diameter >500 m (Figure 3a). The crater retention age estimated from the crater size frequency distribution (CSFD) [6-8] within the ellipse is estimated to be $3.7^{+0.05}_{-0.08}$ Ga for crater diameter >500 m (Figure 3b).

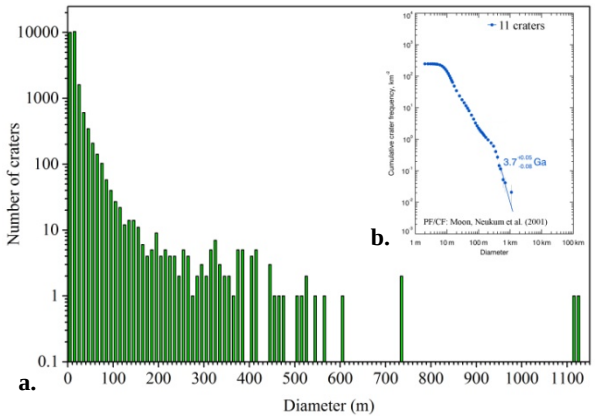

Figure 3. (a) Size-distribution of craters within the landing ellipse. The minimum and maximum diameter of craters present over the landing ellipse is ~2.28 m and ~1.13 km, respectively. (**b)** The inset in Figure 3a shows the crater size frequency distribution derived crater retention age of the landing ellipse.

Spectral analysis. For the spectral analysis (Figure 4), we have used a topographically, photometrically, and thermally corrected Chandrayaan-1 M^3 [9] spectral reflectance mosaic resampled to 300 pixels per degree [10-11]. We have found at least two locations within the landing ellipse that exhibit absorptions at both 1000 nm (band I) and 2000 nm (band II) that suggest the presence of pyroxene (Figure 4).

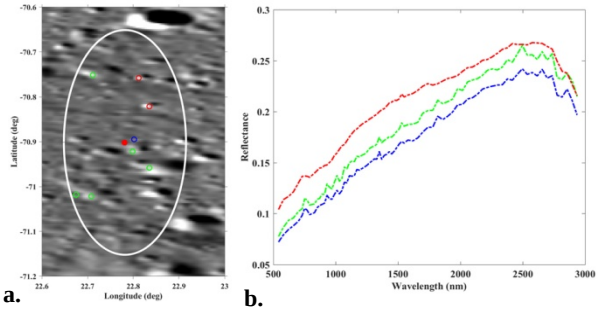

Figure 4. (a) M^3 albedo mosaic (1578 nm) with locations marked for extracted representative reflectance spectra shown in (b). Red circle in the center of landing ellipse (white solid line) shows the location of the PLS. **(b)** The M^3 representative reflectance spectra are shown with the same color as the locations marked in (a). The representative spectrum in blue color is the most common spectral signature within the landing ellipse with no prominent absorption features. The representative spectrum shown in green found at fresh crater locations marked in green in (a). The representative spectrum in red exhibit band I and band II absorption features and found at few craters within landing ellipse as shown in (a).

Composition. For estimating and mapping the distribution of the elements Fe, Mg, and Ca in the landing ellipse, we used the multivariate regression approach proposed by [10, 12-13]. For the element Ti, we used a quadratic polynomial regression approach [13]. The estimated average abundance of elements vary as: Fe: 4.2wt.%, Mg: 5.4wt.%, Ca: 9.9wt.%, and Ti: 0.3wt.%.

Summary: The landing ellipse is generally flat in the LRO WAC DTM ('GLD100' at 100 m/pixel) [14] and is confined by craters of varying diameter. The center of the landing ellipse (i.e., PLS) is devoid of craters with significant depth. The estimated age of the landing ellipse reveals that it is younger than the age of impact craters present to the north (e.g. Manzinus)`. Ejecta of the crater Schomberger in the south superimpose the landing ellipse region. Therefore, it is possible that these craters could have significantly changed the stratigraphy of the landing region. The 1:5,000,000 lunar geologic renovation (2013) map I-703 shows that the geologic unit within the landing ellipse corresponds to unit Ntp (Nectarian plains) [15-16]. Ntp is defined as 'terra mantling and plains material' and is proposed to be sourced by primary and secondary ejecta deposits of Nectarian basins and large craters on the Moon [15]. Therefore, it is likely that the landing ellipse may host primary crustal materials.

Our spectral analysis suggests the presence of weak absorption bands centered at ~900-950 nm and ~2000 nm at two locations within the landing ellipse. This indicates the presence of low-calcium pyroxene. The landing ellipse is mainly dominated by highland-type featureless spectra indicative of FAN lithologies. Our spectral and chemical composition analyses suggest that the surface composition corresponds to FAN materials mixed with Mg-suite rocks. We hypothesize that such a lithology could be a result of mixing of ejecta from the SPA basin impact that may have excavated and redistributed lower crustal or upper mantle materials.

References: [1] Mylswamy, A. et al. (2012) *39th COSPAR Scientific Assembly*, p. 1311. [2] Amitabh et al. (2018) *LPSC XXXXIX*, Abstract #1975. [3] Smith, D.E. et al. (2010) *GRL, 37*, L18204. [4] Robinson, M.S. et al. (2010) *Space Sci. Rev., 150 (1-4)*, 81-124. [5] Haruyama, J. et al. (2012) *LPSC XXXXIII*, Abstract #1200. [6] Kneissl, T. et al. (2011) *Planet. Space Sci., 59*, 1243-1254. [7] Michael, G.G. et al. (2012) *Icarus, 218*, 169-177. [8] Neukum, G. et al. (2001) *Space Sci. Rev., 96(1-4)*, 55-86. [9] Pieters, C.M. et al. (2009) *Current Science, 96*, 500-505. [10] Wöhler, C. et al. (2014) *Icarus, 235*, 86-122. [11] Wöhler, C. et al. (2017) Sci. Adv. 3(9), e1701286. [12] Wöhler, C. et al. (2018) *European Lunar Sym., Toulouse, France*. [13] Bhatt, M. et al. (2015) *Icarus, 248*, 72-88. [14] Scholten, F. et al. (2012) *JGR, 117*, E00H17. [15] Wilhelms, D.E. et al. (1979) *Department of the Interior, US Geological Survey*. [16] Fortezzo, C.M. and Spudis, P.D. (2018) *LPSC XXXXIX*, Abstract #2433.